# Tumor Imaging Using a Picomolar Affinity HER2 Binding Affibody Molecule

Anna Orlova,[1,3] Mikaela Magnusson,[1] Tove L.J. Eriksson,[1] Martin Nilsson,[1] Barbro Larsson,[1] Ingmarie Höidén-Guthenberg,[1] Charles Widström,[2] Jörgen Carlsson,[3] Vladimir Tolmachev,[1,3] Stefan Ståhl,[4] and Fredrik Y. Nilsson[1,3]

[1]Affibody AB, Bromma; [2]Department of Hospital Physics, Uppsala University Hospital; [3]Department of Oncology, Radiology, and Clinical Immunology, Rudbeck Laboratory, Uppsala University, Uppsala; and [4]Department of Biotechnology, AlbaNova University Center, Royal Institute of Technology, Stockholm, Sweden

## Abstract

**The detection of cell-bound proteins that are produced due to aberrant gene expression in malignant tumors can provide important diagnostic information influencing patient management. The use of small radiolabeled targeting proteins would enable high-contrast radionuclide imaging of cancers expressing such antigens if adequate binding affinity and specificity could be provided. Here, we describe a HER2-specific 6 kDa Affibody molecule (hereinafter denoted Affibody molecule) with 22 pmol/L affinity that can be used for the visualization of HER2 expression in tumors *in vivo* using gamma camera. A library for affinity maturation was constructed by re-randomization of relevant positions identified after the alignment of first-generation variants of nanomolar affinity (50 nmol/L). One selected Affibody molecule, $Z_{HER2:342}$ showed a >2,200-fold increase in affinity achieved through a single-library affinity maturation step. When radioiodinated, the affinity-matured Affibody molecule showed clear, high-contrast visualization of HER2-expressing xenografts in mice as early as 6 hours post-injection. The tumor uptake at 4 hours post-injection was improved 4-fold (due to increased affinity) with 9% of the injected dose per gram of tissue in the tumor. Affibody molecules represent a new class of affinity molecules that can provide small sized, high affinity cancer-specific ligands, which may be well suited for tumor imaging.** (Cancer Res 2006; 66(8): 4339-48)

## Introduction

Molecular phenotyping of gene products that are aberrantly expressed in tumors, thus allowing for diagnosis of tumors by targeted visualization of cancer markers (e.g., HER2), holds promise for a shift in clinical practice towards personalizing cancer treatment. However, development has been hampered by the lack of specific agents that bind such gene products, which in addition have properties making them suitable for use as medical imaging agents.

A targeting agent for medical imaging should have high affinity for its target (1) and should be able to specifically target relevant disease-related structures in the body while avoiding normal tissue (2). In the patient, it should quickly find its target whereas unbound molecules should be rapidly excreted, thus facilitating high-contrast tumor imaging and reducing the time between injection and examination. Although antibodies can be selected for good specificity, they are too large to allow for rapid kinetics. Therefore, smaller antibody fragments have gained increasing interest and there are a number of reports on the use of antibody fragments for *in vivo* imaging (3–5). However, further size reduction of these affinity proteins (27-54 kDa) could potentially improve extravasation, increase tissue penetration, and speed up blood clearance (6), thereby increasing imaging contrast. Short peptides, on the other hand, are small and have very rapid kinetics. Natural peptide receptor ligand derivatives, for example, show great potential for radionuclide imaging (7, 8), but there is a limited repertoire of natural peptides to choose from. Unfortunately, peptides derived from screening using phage display libraries seldom have the high affinity necessary to be considered a general class of targeting molecules (9). Therefore, it would be attractive to develop new targeting agents, which are smaller than antibody fragments in order to improve tumor penetration but have better binding specificity and affinity than short peptides. Efforts towards improved affinity proteins have recently been made based on different protein scaffolds (10–12), e.g., "trinectins" (13, 14), "anticalins" (15), "ankyrin repeats" (16), engineered T cell receptors (17), and "Affibody molecules" (18).

Affibody molecules represent a new class of affinity proteins based on a 58–amino acid residue protein domain, derived from one of the IgG-binding domains of staphylococcal protein A. This three-helix bundle domain has been used as a scaffold for the construction of combinatorial phagemid libraries, from which Affibody variants that target the desired molecules can be selected using phage display technology (18, 19). The simple, robust structure of Affibody molecules in combination with their low molecular weight (6 kDa), make them suitable for a wide variety of applications, for instance, as detection reagents (20) and to inhibit receptor interactions (21). In this work, an Affibody molecule specific for HER2 is described.

HER2 is a transmembrane protein belonging to the human epidermal growth factor tyrosine kinase receptor family and is overexpressed in several cancer types, but is present only to a small extent or not at all in normal adult tissue (22, 23). In breast and ovarian cancers, HER2 is overexpressed in 23% to 30% of all cases (24). In patients with breast cancer, the overexpression of HER2 is associated with shorter time to disease progression and decreased overall survival, and it has been shown that the overexpression is preserved in metastases (25, 26). Clinical practice guidelines of the American Society of Clinical Oncology recommend detection of HER2 expression in all newly diagnosed or recurrent breast carcinomas in order to select patients who will benefit from

**Note:** A. Orlova and M. Magnusson contributed equally to this study.

**Requests for reprints:** Fredrik Y. Nilsson, Affibody AB, Box 20137, SE-161 02 Bromma. Phone: 46-8-5988-3851; Fax: 46-8-5988-3801; E-mail: fredrik.nilsson@affibody.se.



doi:10.1158/0008-5472.CAN-05-3521

treatment with Herceptin and anthracyclines (27). The use of radionuclide molecular imaging of HER2 expression may help to rapidly identify HER2 expression in tumor lesions, it may assist to avoid false-negative results due to sampling errors and heterogeneity of expression from biopsy probes, and can provide information on HER2 expression in cancers resistant to trastuzumab treatment. Together, these factors provide strong arguments for the development of radionuclide targeting strategies directed against HER2.

A previously selected Affibody molecule, $Z_{HER2:4}$ (28), was shown to bind selectively to the extracellular domain of HER2 with an affinity of 50 nmol/L. Literature data shows that an increase of affinity beyond $10^{-8}$ mol/L improves the tumor uptake of targeting proteins (29, 30). To increase the affinity, we tried dimerization of $Z_{HER2:4}$ (31, 32) and affinity maturation by directed evolution, as reported here. For antibodies, secondary libraries for affinity maturation have proven successful in generating high-affinity scFv binders to HER2 (e.g., 13 pmol/L; ref. 33). However, to this date, it has not been shown whether single domain scaffold proteins, such as the 6 kDa Affibody molecule, could yield such high-affinity binders. Here, we describe a monovalent HER2-binding Affibody molecule with a 2,200-fold increased affinity obtained through an affinity maturation process of the parental binder (28). The binder was characterized *in vitro* and *in vivo* and compared with the nanomolar parental molecule. Tumor imaging efficiency was shown in mice using gamma camera.

## Materials and Methods

**Construction of a secondary phagemid library.** The secondary library was created by PCR amplification from a single 129-nucleotide template oligonucleotide with certain degenerated codons (5′-ctc gag gta gac aac aaa ttc aac aaa gaa nnk mrm mmm gcg tat tgg gag atc nnk nnk tta cct aac tta aac nnk nnk caa nnk cgc gcc ttc atc cgc agt tta tat gat gac cca agc caa agc-3′), encoding helices 1 and 2 of the Z domain. The gene fragment was amplified using the forward primer 5′ccccccccctcgaggtaga caacaaattcaa-5′ (*Xho*I site underlined) and the reverse primer 5′ccccctgctagcaagttagcgctttggcttgggtcatc-3′ (*Nhe*I site underlined), with 100 fmol template oligonucleotide for each of 95 parallel reactions. The amplifications were done using AmpliTaq Gold polymerase (Applied Biosystems, Foster City, CA) for 10 cycles (15 seconds at 96°C, 15 seconds at 60°C, and 1 minute at 72°C), pooled, purified using the QIAquick PCR purification kit (Qiagen, Hilden, Germany), *Xho*I/*Nhe*I digested and ligated to *Xho*I/*Nhe*I-phagemid vector pAffi1[28] encoding the third nonvariegated α-helix of the Z domain. Electrocompetent *Escherichia coli* RRIΔM15 (34) cells were transformed with 60 aliquots of ligated material using 0.2-cm gap size cuvettes in an ECM 630 set (BTX, Genetronics) at 2,500 V, 125 Ω and 50 μF. Cells were grown in SOC medium [tryptone soy broth (TSB) + yeast extract (YE) supplemented with 1% glucose, 10 mmol/L $MgCl_2$, 10 mmol/L $MgSO_4$, 10 mmol/L NaCl, and 2.5 mmol/L KCl] for 50 minutes and transferred to six Erlenmayer flasks, each containing 1 L of TSB + YE (30 g/L TSB and 5 g/L YE; both from Merck, Darmstadt, Germany) supplemented with 2% glucose and 25 μg/mL carbencillin and grown overnight at 37°C. The cells were centrifuged at 2,000 × *g*, following resuspension in PBS/glycerol solution to a final approximate concentration of 20% glycerol, aliquoted and stored at −80°C.

**Phage selection procedures.** Preparation of phage stocks from the affinity maturation library (a portion of $Zlib2004_{HER2mat}$) and between selections was done according to previously described procedures (18) using the helper phage M13K07 (New England Biolabs, Beverly, MA). Polyethylene glycol/NaCl precipitation yielded phage titers of ~$10^{13}$ colony-forming units/mL. A 100 kDa recombinant extracellular domain of HER2 (HER2-ECD) comprising 624 amino acids (35), corresponding to nucleotides 238 to 2,109, was used as target proteins during selection. The protein was biotinylated as previously described (25) using EZ-Link Sulfo-NHS-LC-Biotin (Pierce, Rockford, IL) with a 30 times molar excess of biotin.

The library was subjected to five rounds of selection in solution on biotinylated HER2-ECD using a 10-fold decreasing target concentration for each round. To avoid nonspecific binders, all tubes used in this procedure were pretreated with PBST supplemented with 0.1% gelatin and the phage stock/s were preincubated with streptavidin beads (Dynabeads M-280 Streptavidin; 112.06, Dynal A.S., Oslo, Norway) for rounds 1 and 2. The phage library was subjected to biopanning against HER2-ECD for 1 hour and 45 minutes at room temperature under continuous rotation. To capture phage binding biotinylated target, SA beads were incubated with the phage-target mixtures for 15 minutes. The beads were washed and the bound phages were subsequently eluted and propagated as previously described (36, 37).

**ELISA-based ranking of second generation binders.** Single colonies were inoculated in 1 mL TSB-YE medium supplemented with 100 μmol/L isopropyl-L-thio-β-D-galactopyranoside and 100 μg/mL ampicillin in deep well plates (Nunc, Roskilde, Denmark), and grown on a shaker overnight at 37°C. Cells were pelleted by centrifugation at 3,000 × *g* for 10 minutes. The pellets were resuspended in 300 μL PBST and frozen for 30 minutes at −80°C. The samples were thawed and centrifuged at 3,500 × *g* for 20 minutes. The supernatants (100 μL), containing ABD-tagged (38) Affibody molecules were loaded in microtiter wells, which had been previously coated with 6 μg/mL HSA in 15 mmol/L $Na_2CO_3$ and 35 mmol/L $NaHCO_3$ (pH 9.6) overnight at 4°C and blocked with 2% skimmed milk powder in PBST for 1 hour at room temperature. The plates were washed four times with PBST prior to the addition of 100 μL of 1 μg/mL biotinylated HER2 per well and incubated for 1.5 hours. After washing the wells four times, 100 μL streptavidin-horseradish peroxidase (1:5,000; DAKO Cytomation, Denmark) per well were added and incubated for 1 hour. The wells were washed four times and 100 μL developing solution ImmunoPure TMB substrate kit (Pierce) was added to each well. After 30 minutes, 100 μL of the stop solution (2 mol/L $H_2SO_4$) was added to each well. The absorbance at 450 nm was measured in an ELISA reader.

**DNA sequencing and sequence clustering.** DNA sequencing was done with ABI PRISM dGTP, BigDye Terminator v3.0 Ready Reaction Cycle Sequencing Kit (Applied Biosystems) according to the manufacturer's recommendations. The sequences were analyzed on an ABI PRISM 3100 Genetic Analyser.

The Affibody molecules were clustered using the so-called average-link hierarchical clustering method. Initially, each molecule's sequence was defined as a separate subset. A complete clustering was obtained by finding the two subsets that were least dissimilar to each other and selected subsets were merged to create a new subset, decreasing the number of subsets by one. This procedure was repeated until all subsets were clustered. A subset was regarded as a cluster when it showed up as a node relatively close to the vertical axis in a dendrogram, whereas the length of the branch to its parent was relatively large. Cluster validation was done by applying the so-called Nearest-Exterior-Neighbor/Furthest-Interior-Neighbor cluster validation method to the subset output from the clustering method. First, a cluster quality index was computed for each subset. A high value of this index indicates a compact and isolated subset. In a second step, a reference distribution of cluster quality indices was created, against which the cluster quality indices for the obtained subset were compared. This comparison also took subset size into account. The outcome of these comparisons was a number, the so-called significance value, for each subset.

**Protein expression and purification.** Gene fragments encoding the selected second-generation Affibody molecules $Z_{HER2:473}$, $Z_{HER2:382}$, $Z_{HER2:470}$, $Z_{HER2:487}$, $Z_{HER2:489}$, $Z_{HER2:477}$, $Z_{HER2:492}$, $Z_{HER2:475}$, $Z_{HER2:342}$, and $Z_{HER2:336}$, as well as the first-generation binder, $Z_{HER2:4}$ (28), were subcloned from the phagemid vector to a pET-derived expression vector pAY442 under the control of the T7 promoter. The proteins were expressed in *E. coli* BL21(DE3) cells and the $His_6$-tagged proteins were IMAC purified under denatured conditions using QIAfilter 96 Plates Ni-NTA Superflow kit and

QIAsoft 4.1, medium-scale protein/Ni-NTA Superflow 96 Denat program on a Biorobot 3000 (Qiagen). The protein samples refolded when dialyzed in PBS using Slide-A-Lyzer (Pierce) according to the manufacturer's recommendations. The protein concentrations were calculated from the measured absorption values at 280 nm. Extinction coefficients were theoretically calculated from the primary amino acid sequence.

**Biosensor analyses.** A BIAcore 2000 instrument (Biacore AB, Uppsala, Sweden) was used for real-time biospecific interaction analysis between selected Affibody molecules and the target protein. HER2-ECD [diluted in 10 mmol/L NaAc (pH 4.5)] was immobilized (~3,500 resonance units) on a CM5 sensor chip (BR-1000-14, Biacore) according to the manufacturer's instructions. Another flow-cell surface was activated and deactivated to be used as a reference surface, and human IgG (Amersham Biosciences) was immobilized (~5,000 resonance units) on a separate flow-cell surface on CM5 sensor chips, to serve as negative controls. Binding analyses were done at 25°C, and PBS was used as the running buffer. In a first experiment, 50 nmol/L of each Affibody molecule (diluted in PBS) was injected over all surfaces with a flow rate of 10 μL/min.

In a second experiment, the $Z_{HER2:342}$ and $Z_{HER2:477}$ Affibody variants were subjected to a kinetic analysis, in which the proteins were injected over a HER2-ECD surface (approximate immobilization levels of 1,200, 1,600, and 2,000 resonance units, respectively) at different concentrations (0-6 nmol/L, with 0.19 nmol/L as the lowest protein concentration diluted in PBS) with a flow rate of 50 μL/min. The dissociation equilibrium constant

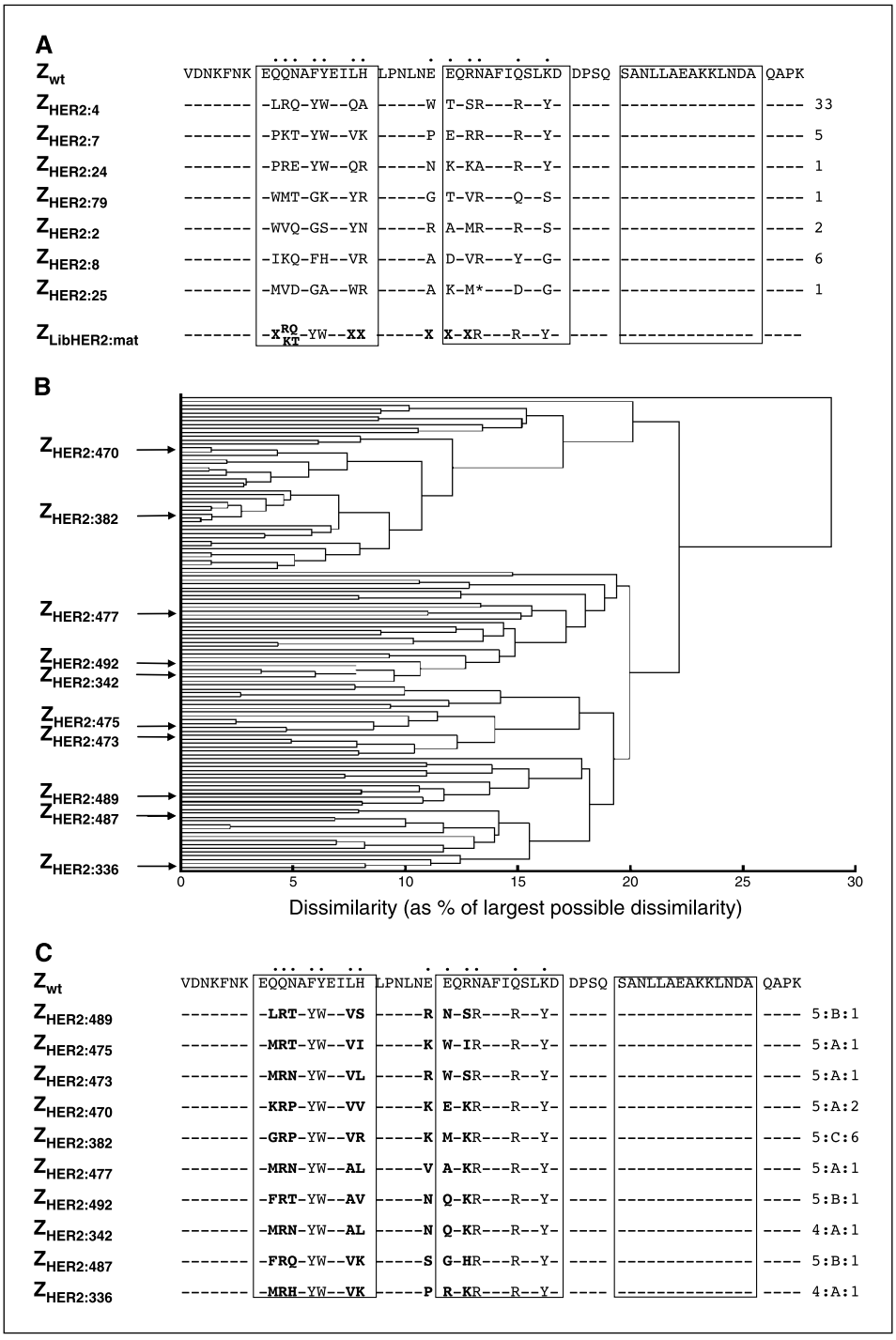


**Figure 1.** *A,* the strategy for affinity maturation. Amino acid sequence of the wild-type Z domain aligned to deduced amino acid sequences of different Affibody variants selected against HER2-ECD (28). The 13 randomized amino acid residues (Q9, Q10, N11, F13, Y14, L17, H18, E24, E25, R27, N28, Q32, and K35) are presented. An amber stop codon is included in the $Z_{HER2:25}$ variant. *Horizontal bars,* amino acid identities. *Right,* the number of times each variant was found upon DNA sequencing of 49 colonies. The design of the constructed library aimed for affinity maturation ZLibHER2:mat is presented in single letter code, with positions selected for variation in boldface (X = any amino acid). Note, that a bias for arginine or lysine residues is introduced at position 10, and a bias for glutamine or threonine residues at position 11. The three α-helices in the wild-type Z domain are boxed. *B,* sequence clustering. The Affibody molecules were clustered using an average-link hierarchical clustering method, and the result is illustrated in a dendrogram. A subset was regarded as a cluster when it showed up as a node relatively close to the vertical axis in the dendrogram, whereas the length of the branch to its parent was relatively large. Cluster validation was done by applying a Nearest-Exterior-Neighbor/Furthest-Interior-Neighbor cluster validation method to the subset output from the clustering method. Positions of the 10 second-generation Affibody molecules selected for further characterization. *C,* sequences of selected second-generation Affibody variants. Amino acid sequence of the wild-type Z domain aligned to deduced amino acid sequences of 10 different second-generation Affibody variants selected in the affinity maturation effort against HER2-ECD. The amino acid residues found in the variegated position in boldface. Amino acid residues other than R/K at position 10 and Q/T at position 11 could appear by alternative combinations of the included nucleotides. *Right,* the selection cycle from which the clone was isolated/the selection principle applied for this specific clone/the number of times each variant was found on DNA sequencing of 160 randomly picked colonies from selection cycles four and five.

($K_D$), the association rate constant ($k_a$), and the dissociation rate constant ($k_d$) were calculated using BIAevaluation 3.2 software (Biacore), assuming a one-to-one Langmuir binding model taking mass transfer effects into account. A long dissociation phase was applied (60 minutes), due to the slow off rate, to get fully reliable results.

In a third experiment, the difference in binding to HER2-ECD between the monovalent $Z_{HER2:4}$ (28) and the divalent $(Z_{HER2:4})_2$ (31) first-generation Affibody variants and the affinity-matured second-generation $Z_{HER2:342}$ Affibody molecule, was evaluated by injection of 5 μmol/L of each protein over the HER2-ECD surface, with a flow rate of 5 μL/min.

**Immunofluorescence.** The human ovarian adenocarcinoma SKOV-3 (HTB-77, ATCC), and the human neuroblastoma cell line, SH-SY5Y (CRL-2266, ATCC), were grown in 5% $CO_2$ incubator at 37°C in 25 $cm^2$ flasks. SKOV-3 cells were cultured in McCoy's 5a and SH-SY5Y in DMEM medium (Life Technologies, Invitrogen) supplemented with 2 mmol/L glutamine and 10% fetal calf serum (Life Technologies, Invitrogen). Cells were trypsinated (Trypsin-EDTA, Life Technologies, Invitrogen) the day before analysis, washed in medium, and resuspended to a concentration of $2.5 \times 10^5$ cells/mL. Approximately 5,000 to 10,000 cells were added per well of an eight-well, multi-well slide (Histolab, Sweden). The cells were incubated on multi-well slides overnight to obtain a flat morphology. The next day, medium was gently removed from the slides and cells were stained for 1 hour with the $Z_{HER2:342}$ Affibody molecule (5 μg/mL) or 0.5 μg/mL of the monoclonal antibody trastuzumab (Herceptin, Apoteket AB, Sweden), with a volume of 20 μL/well. After staining, cells were fixed with 3% formaldehyde in PBS, one drop per well for 15 minutes. The slides were rinsed in PBS and the $Z_{HER2:342}$ Affibody molecule was detected with mouse anti-Affibody mouse serum (prepared in-house) followed by 5 μg/mL of goat anti-mouse IgG Alexa Fluor 488 (Molecular Probes, Eugene, OR). Trastuzumab was detected with 5 μg/mL of goat anti-human IgG Alexa Fluor 488 (Molecular Probes). The slides were counterstained with 20 μL of 4′,6-diamidino-2-phenylindole (Molecular Probes), 1 μg/mL for 5 seconds, washed, dried for 1 hour, and mounted with antifading reagent (Vector Laboratories, Inc.).

$Z_{HER2:342}$ and anti-HER2 antibody were used to simultaneously stain HER2 on SKOV-3 cells. Slides with formaldehyde-fixed cells were stained with $Z_{HER2:342}$ (5 μg/mL) Affibody molecule followed by goat anti-Affibody IgG and rabbit anti-goat IgG Alexa Fluor 488 (Molecular Probes). Antibody staining was done on Affibody molecule–stained cells and the antibody was detected with anti-human IgG Alexa Fluor 555 as described above. The slides were counterstained with 20 μL of 4′,6-diamidino-2-phenylindole (Molecular Probes), 1 μg/mL for 5 seconds, washed, dried for 1 hour, and mounted with antifading reagent (Vector Laboratories).

Membrane fluorescence was analyzed in a DMLA microscope, equipped with a digital camera (Leica Microsystems AG). Digital images of green, red and blue fluorescence were acquired and saved as overlays using the IM1000 software (Leica Microsystems).

**Immunohistochemical staining.** SKOV-3 xenograft tumors (described below) were excised and snap-frozen in liquid nitrogen. Six-micron-thick cryosections of the tumors (Ljung CM3000, Leica Microsystems) were fixed in 3% formaldehyde in PBS for 15 minutes and blocked in 1% FCS in PBS for 1 hour before staining. The sections were either stained with $Z_{HER2:342}$ at a concentration of 5 μg/mL, followed by polyclonal rabbit anti-Affibody IgG (prepared in-house) and horseradish peroxidase-conjugated anti-rabbit IgG (DAKO Cytomation) or with trastuzumab (0.5 μg/mL) followed by horseradish peroxidase–conjugated anti-human IgG (DAKO Cytomation). The staining was developed for 7 minutes with 3,3′-diaminobenzidine chromogen substrate (DAKO Cytomation) and then washed for 2 to 3 minutes. The slides were counterstained with Mayers HTX (Histolab) for 20 seconds and then rinsed for 10 minutes before mounting with Mount-quick (Histolab). The staining was analyzed in a DMLA microscope, equipped with a digital camera (Leica Microsystems). Digital images were acquired and saved using the IM1000 software (Leica Microsystems).

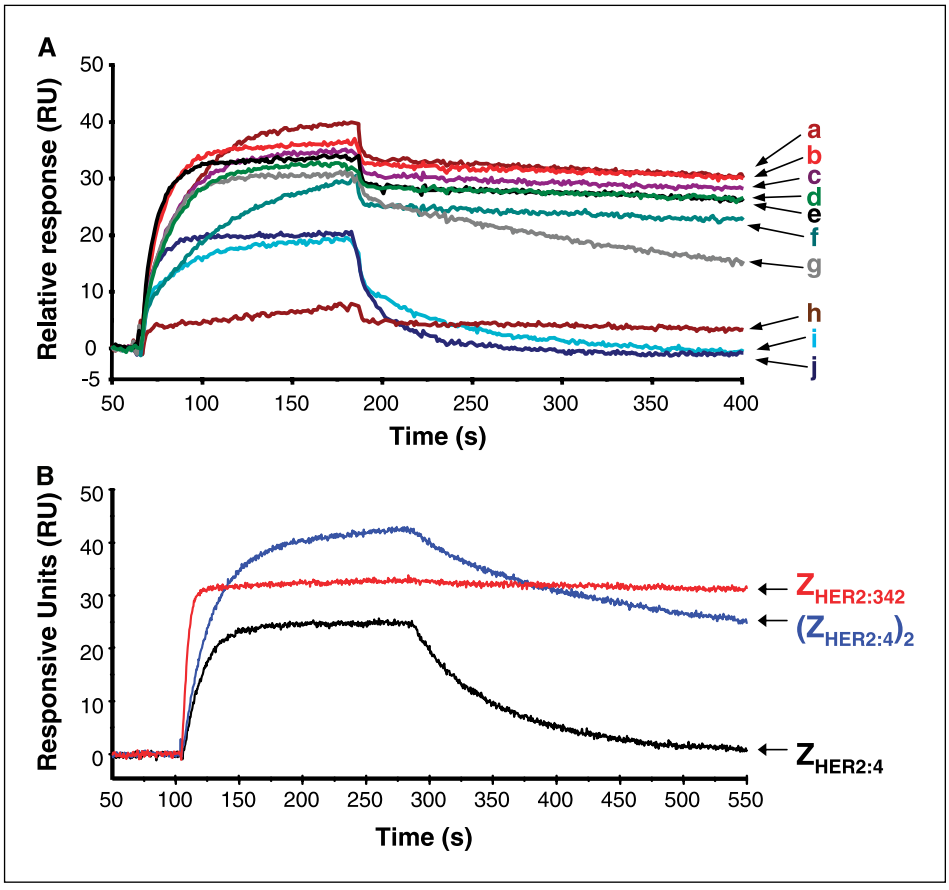


**Figure 2.** Biacore ranking of second-generation Affibody variants and comparison to first generation binders. *A,* sensorgrams obtained after injection of the 10 different second-generation Affibody molecules over a sensor chip flow-cell surface containing amine-coupled HER2-ECD. Sensorgrams are: (*a*) $Z_{HER2:336}$, (*b*) $Z_{HER2:342}$, (*c*) $Z_{HER2:475}$, (*d*) $Z_{HER2:477}$, (*e*) $Z_{HER2:492}$, (*f*) $Z_{HER2:487}$, (*g*) $Z_{HER2:489}$, (*h*) $Z_{HER2:473}$, (*i*) $Z_{HER2:382}$, and (*j*) $Z_{HER2:470}$. *B,* sensorgrams obtained after injection of monovalent $Z_{HER2:4}$ Affibody molecule, compared with divalent $(Z_{HER2:4})_2$ Affibody molecule and second-generation $Z_{HER2:342}$ Affibody molecule over a sensor chip containing amine-coupled HER2-ECD.

**Radioiodination.** The radiolabeling with $^{125}$I of the $Z_{HER2:342}$ Affibody molecule was done using *N*-succinimidyl *p*-(trimethylstannyl)benzoate as a precursor, as previously described (25). Labeling conditions were adjusted to provide attachment for a single prosthetic group per protein molecule. Radiochemical purity was controlled using ITCL SG eluted with 70% acetone in water and was always better than 95%. The radiolabeled Affibody molecules were analyzed using Biacore technology to verify that the labeling procedure had not affected the binding affinity to HER2-ECD.

**Biodistribution in tumor-bearing mice.** Animal experiments were approved by the local ethics committee for animal research. SKOV-3 xenografts were established on female BALB/c *nu/nu* mice (10-12 weeks old on arrival), 4 to 8 weeks before the experiment by implanting $\sim 5 \times 10^6$ cells s.c. on the right hind leg. All mice were injected with $\sim 50$ μL (0.5 μg, 100 kBq) of the $^{125}$I-labeled $Z_{HER2:4}$, $(Z_{HER2:4})_2$, or $Z_{HER2:342}$ Affibody molecules into the tail vein. Groups of four mice were sacrificed after 1, 4, and 24 hours, and organs were dissected, weighted, and their radioactivity content was measured in the automated gamma counter. Tissue uptake was calculated as the percentage of injected radioactivity per gram of tissue (% IA/g). To show that tumor uptake was target-mediated, a control group of four animals was pretreated with 0.5 mg of cold, nonlabeled Affibody molecules 45 minutes before the injection of 0.5 μg of the radioiodinated counterpart. Four hours later, these animals were sacrificed and tumor radioactivity uptake was measured.

**Gamma camera–based imaging.** SKOV-3 xenografts were established for $\sim 2$ months, as described above. The tumors had an average volume of $\sim 0.5$ cm$^3$ at the day of the experiment. In total, 60 μg of $Z_{HER2:342}$ was labeled with 111 MBq $^{125}$I, resulting in a specific activity of 1.3 MBq/μg. Each mouse was injected with 90 μL (2.3 μg, 2.9 MBq) $^{125}$I-$Z_{HER2:342}$. After 6 or 24 hours, respectively, mice were euthanized with a lethal dose of Ketalar/Rompun i.p. The mice were imaged using an e.CAM gamma camera (Siemens, Erlangen, Germany) with a low-energy high-resolution collimator.

## Results

**Affinity maturation of first-generation HER2 binders.** We designed and constructed the affinity maturation library based on a primary set of HER2-binding Affibody molecules (28). These were aligned with an allowed bias for the strongest binders, and we found it reasonable to fix 5 (13, 14, 28, 32, and 35), and allow a bias for R and K in position 10, and Q and T in position 11, of the 13 originally randomized amino acid residues. Thus, positions 9, 17, 18, 24, 25, and 27 were targeted for randomization (Fig. 1*A*) using NNG/T degenerated codons. Due to the small size of the Affibody molecule, it was possible to use a single 129 nucleotide oligonucleotide with degenerated codons, encoding helices 1 and 2 of the Z-domain, to create the secondary library. The oligonucleotide was PCR-amplified and subsequently ligated into a phagemid vector encoding the third α-helix of the Z-domain. The resulting library consisted of $\sim 3 \times 10^8$ members, which should be enough to sample a majority of all theoretical variants. Phage stocks were prepared and selections done essentially as previously described (18, 28), using decreasing concentrations of target protein and intensive washing to select for the strongest HER2-binding Affibody variants in the library.

Clones obtained after four and five rounds of selection were cultivated in 96-well plates, freeze-thawed to release periplasmic content, and subjected to an ELISA screening procedure for HER2 binding activity (data not shown). When subjecting 160 randomly picked clones to this ELISA screening, using the first-generation Affibody molecule $Z_{HER2:4}$ as reference, a majority of the clones gave significantly higher absorbance values than the reference $Z_{HER2:4}$, thus, indicating stronger HER2 binding (data not shown). The same 160 clones were subjected to DNA sequencing, and upon clustering of the sequenced clones using an average-link hierarchical clustering method developed in-house, the relationship between selected clones was visualized (Fig. 1*B*). Based on the values in the ELISA screening and the clustering results, 10 clones were selected for further characterization (Fig. 1*C*). The cycle from which the particular clone was isolated, and the frequency of occurrence are indicated (Fig. 1*C*), as well as their position in the clustering analysis (Fig. 1*B*).

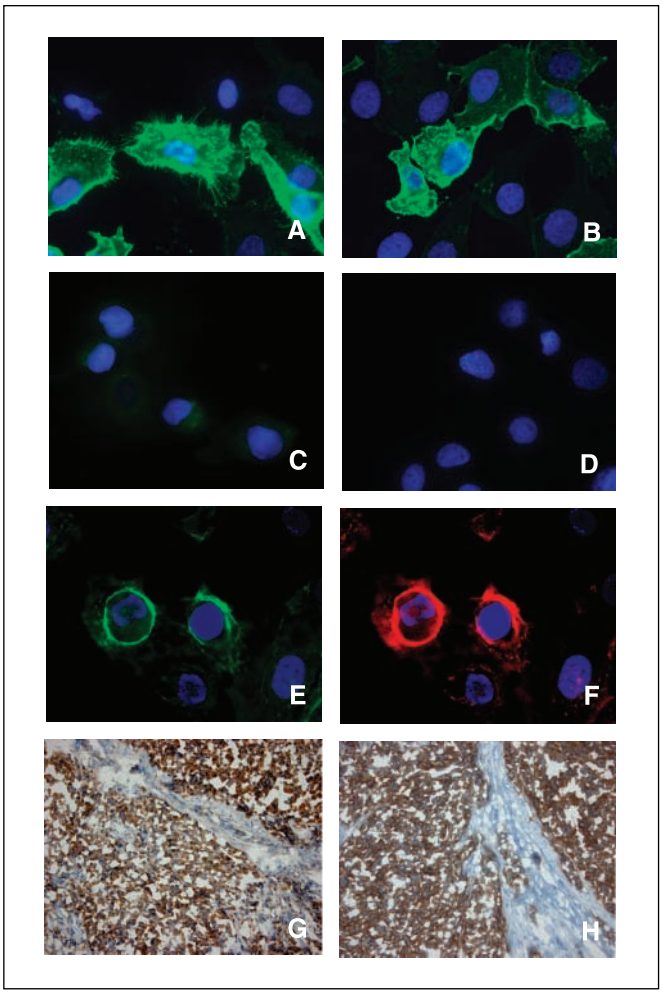


**Figure 3.** Fluorescence staining of SKOV-3 and SH-SY5Y cells with $Z_{HER2:342}$ and trastuzumab. *A,* SKOV-3 cells stained for HER2 expression with $Z_{HER2:342}$ Affibody molecules; *B,* SKOV-3 cells stained for HER2 expression with trastuzumab; *C,* the HER2-negative cell line SH-SY5Y stained with $Z_{HER2:342}$; and *D,* the HER2-negative cell line SH-SY5Y stained with trastuzumab. *E* and *F,* the same cells double-stained for $Z_{HER2:342}$ (*green*) and trastuzumab (*red*), respectively. *G,* immunohistochemical staining of HER2 with $Z_{HER2:342}$ Affibody molecules was done on a section of SKOV-3 cell xenograft tumor. The section was counterstained with hematoxylin (*blue*). The transversing mouse connective tissue remains negative. *H,* a consecutive section of SKOV-3 cell xenograft tumor was stained with trastuzumab.

**Biosensor screening, stability, and affinity determination.** To obtain an initial ranking of binding affinities, the 10 selected Affibody variants as well as the $Z_{HER2:4}$ and dimeric $(Z_{HER2:4})_2$ were expressed and analyzed for their HER2 binding using a Biacore instrument. The different Affibody molecules were separately injected over sensor chip flow-cell surfaces containing the immobilized target protein HER2-ECD and a control protein IgG, respectively. An overlay plot of the obtained sensorgrams suggested

**Table 1.** Biodistribution of $Z_{HER2:4}$, $(Z_{HER2:4})_2$, and $Z_{HER2:342}$

| Organ (% IA/g) | 1 hour | | | 4 hours | | | 24 hours | | |
|---|---|---|---|---|---|---|---|---|---|
| | $Z_{HER2:4}$ | $(Z_{HER2:4})_2$ | $Z_{HER2:342}$ | $Z_{HER2:4}$ | $(Z_{HER2:4})_2$ | $Z_{HER2:342}$ | $Z_{HER2:4}$ | $(Z_{HER2:4})_2$ | $Z_{HER2:342}$ |
| Blood | 2.61 ± 0.35 | 3.83 ± 0.29 | 4.50 ± 0.78 | 0.39 ± 0.09 | 0.56 ± 0.14 | 0.25 ± 0.03 | 0.03 ± 0.00 | 0.02 ± 0.01 | 0.04 ± 0.01 |
| Heart | 1.00 ± 0.16 | 1.34 ± 0.12 | 2.11 ± 0.64 | 0.13 ± 0.06 | 0.31 ± 0.14 | 0.11 ± 0.02 | 0.01 ± 0.00 | 0.01 ± 0.01 | 0.01 ± 0.02 |
| Lung | 2.25 ± 0.40 | 2.56 ± 0.10 | 4.56 ± 1.02 | 0.40 ± 0.09 | 0.44 ± 0.12 | 0.37 ± 0.03 | 0.04 ± 0.01 | 0.05 ± 0.02 | 0.07 ± 0.02 |
| Liver | 4.08 ± 0.70 | 5.10 ± 0.25 | 8.32 ± 1.18 | 0.77 ± 0.09 | 1.00 ± 0.38 | 0.30 ± 0.05 | 0.07 ± 0.03 | 0.02 ± 0.00 | 0.04 ± 0.00 |
| Spleen | 1.81 ± 0.40 | 1.41 ± 0.10 | 2.68 ± 0.37 | 0.58 ± 0.17 | 0.19 ± 0.04 | 0.12 ± 0.02 | 0.06 ± 0.03 | 0.01 ± 0.01 | 0.03 ± 0.01 |
| Pancreas | 0.93 ± 0.10 | 2.43 ± 0.08 | 2.48 ± 0.48 | 0.16 ± 0.06 | 0.26 ± 0.05 | 0.13 ± 0.03 | 0.01 ± 0.00 | 0.02 ± 0.01 | 0.01 ± 0.00 |
| Kidney | 24.98 ± 3.69 | 68.90 ± 10.62 | 49.64 ± 6.72 | 6.04 ± 0.64 | 29.85 ± 3.16 | 9.51 ± 0.78 | 0.16 ± 0.01 | 0.87 ± 0.13 | 0.46 ± 0.21 |
| Stomach | 1.18 ± 0.10 | 2.26 ± 0.29 | 2.21 ± 0.46 | 0.59 ± 0.30 | 0.76 ± 0.21 | 0.25 ± 0.04 | 0.02 ± 0.00 | 0.06 ± 0.08 | 0.03 ± 0.01 |
| Small intestine | 2.35 ± 0.70 | ND ± ND | 2.65 ± 1.01 | 0.41 ± 0.13 | ND ± ND | 0.61 ± 0.27 | 0.01 ± 0.01 | ND ± ND | 0.01 ± 0.01 |
| Large intestine | 0.90 ± 0.15 | ND ± ND | 1.93 ± 0.67 | 0.12 ± 0.06 | ND ± ND | 0.66 ± 0.50 | 0.00 ± 0.00 | ND ± ND | 0.01 ± 0.01 |
| Salivary glands | 1.33 ± 0.18 | 2.70 ± 0.53 | 2.33 ± 0.27 | 0.60 ± 0.14 | 1.39 ± 0.31 | 0.33 ± 0.09 | 0.02 ± 0.00 | 0.03 ± 0.02 | 0.02 ± 0.02 |
| Skin | 1.33 ± 0.24 | 3.31 ± 1.18 | 2.58 ± 0.75 | 0.25 ± 0.07 | 0.27 ± 0.09 | 0.26 ± 0.10 | 0.02 ± 0.00 | 0.02 ± 0.01 | 0.03 ± 0.01 |
| Muscle | 0.36 ± 0.06 | 0.84 ± 0.12 | 0.66 ± 0.14 | 0.05 ± 0.02 | 0.07 ± 0.03 | 0.06 ± 0.03 | 0.00 ± 0.00 | ND ± ND | 0.00 ± 0.00 |
| Bone | 0.54 ± 0.08 | 0.56 ± 0.11 | 1.03 ± 0.24 | 0.06 ± 0.05 | 0.08 ± 0.04 | 0.11 ± 0.02 | 0.00 ± 0.00 | 0.05 ± 0.04 | 0.03 ± 0.04 |
| Brain | 0.07 ± 0.01 | ND ± ND | 0.12 ± 0.02 | 0.00 ± 0.00 | ND ± ND | 0.04 ± 0.02 | 0.00 ± 0.00 | ND ± ND | 0.00 ± 0.00 |
| Tumor | 4.05 ± 1.28 | 3.23 ± 0.12 | 8.23 ± 2.08 | 2.40 ± 0.17 | 2.27 ± 0.55 | 9.46 ± 1.60 | 0.17 ± 0.03 | 0.34 ± 0.11 | 4.13 ± 0.46 |
| Ratios | | | | | | | | | |
| Tumor/blood | 1.6 | 0.8 | 1.8 | 6.2 | 4.1 | 37.8 | 5.7 | 17.0 | 103.3 |
| Tumor/kidney | 0.2 | 0.0 | 0.2 | 0.4 | 0.1 | 1.0 | 1.1 | 0.4 | 9.0 |
| Tumor/liver | 1.0 | 0.6 | 1.0 | 3.1 | 2.3 | 31.1 | 2.5 | 17.0 | 103.3 |

NOTE: Tumor and normal organ uptakes are expressed as the percentage of injected activity per gram ± SD ($n$ = 4).

that approximately half of the analyzed Affibody variants bound to the target with significantly higher affinities than $Z_{HER2:4}$ (Fig. 2*A*). The slower off-rate kinetics of second-generation variants could clearly be seen by visual inspection of the sensorgrams. As expected, no significant binding could be seen in the control protein IgG (data not shown). A group of four Affibody variants, $Z_{HER2:336}$, $Z_{HER2:342}$, $Z_{HER2:475}$, and $Z_{HER2:477}$, with good binding profiles were selected for further studies.

Differences in solubility between the Affibody variants was investigated. The threshold was set at no loss of protein at a concentration of 4 mg/mL upon freezing and thawing, and with no signs of aggregates in gel filtration (data not shown). $Z_{HER2:336}$ and $Z_{HER:475}$ did not meet these criteria. The melting temperatures ($T_m$'s) of the selected Affibody variants varied substantially: 73°C for $Z_{HER2:336}$, 67°C for $Z_{HER2:342}$, 46°C for $Z_{HER2:475}$, and 49°C for $Z_{HER2:477}$, respectively. The Affibody variants were also tested *in vivo* for tumor uptake and kidney retention at 4 hours with tumor to blood ratios for $Z_{HER2:336}$, $Z_{HER2:342}$, $Z_{HER2:475}$, and $Z_{HER2:477}$ of 18 ± 6, 40 ± 3, 18 ± 4, and 21 ± 6, respectively, and tumor to kidney ratios of 0.6 ± 0.2, 1.0 ± 0.1, 0.5 ± 0.2, and 0.62 ± 0.06, respectively. Taking these different factors into account, the $Z_{HER2:342}$ followed by the $Z_{HER2:477}$ variant seemed to be most promising for further studies.

The $Z_{HER2:342}$ and $Z_{HER2:477}$ Affibody molecules were subjected to a kinetic analysis in order to determine the kinetic binding constants. Prior to the kinetic analysis, the protein concentration was carefully determined by amino acid analysis, and gel filtration was done (data not shown) to confirm a monomeric state. The Affibody molecules were then injected over a HER2-ECD flow-cell surface or a control EGFR-ECD flow-cell surface at different concentrations, and the dissociation equilibrium constant ($K_D$) for HER2-ECD was determined to be ~22 pmol/L for $Z_{HER2:342}$ and ~32 pmol/L for $Z_{HER2:477}$. The association rate constant ($k_a$) was calculated to be $\sim 4.8 \times 10^6$ $M^{-1}$ $s^{-1}$ and the dissociation rate constant ($k_d$) $\sim 1.1 \times 10^{-4}$ $s^{-1}$ for $Z_{HER2:342}$, and for $Z_{HER2:477}$, the $k_a$ was $\sim 4.3 \times 10^6$ $M^{-1}$ $s^{-1}$ and the $k_d$ was $\sim 1.4 \times 10^{-4}$ $s^{-1}$. None of the Affibody molecules bound EGFR-ECD (HER1), a protein which has strong homology with HER2. Based on these data, $Z_{HER2:342}$ was selected for further characterization.

**Comparing first- and second-generation binders *in vitro*.** The affinity-matured $Z_{HER2:342}$ ($K_D$ ~22 pmol/L for HER2) was compared with a monovalent ($K_D$ ~50 nmol/L for HER2) and a divalent form ($K_D$ ~3 nmol/L for HER2) of the first-generation Affibody molecule (28, 31), $Z_{HER2:4}$ using Biacore analysis (Fig. 2*B*). The monovalent and bivalent first-generation Affibody molecule had similar association rates (31), whereas the bivalent $(Z_{HER2:4})_2$ had a 13-fold slower dissociation rate. Interestingly, the affinity-matured $Z_{HER2:342}$ Affibody molecule did not only have a 90-fold slower dissociation rate than the parental $Z_{HER2:4}$, but also a 27-fold faster association rate (Fig. 2*B*).

**Fluorescence and immunohistochemical analysis.** The ability of the matured Affibody molecules to detect membrane-bound HER2 was analyzed using fluorescence microscope analysis. The Affibody molecule $Z_{HER2:342}$ molecule worked very well as a detection reagent and gave a membrane staining on HER2-positive SKOV-3 cells (Fig. 3*A*), but not on HER2-negative SH-SY5Y cells (Fig. 3*C*). Approximately 50% of the SKOV-3 cells were strongly stained with $Z_{HER2:342}$ with an almost identical staining pattern as the monoclonal antibody trastuzumab, which was used as a positive control (Fig. 3*B* and *D*). Double staining with trastuzumab and $Z_{HER2:342}$ Affibody molecules showed that both reagents bind to the same cells and with identical staining morphology

(Fig. 3*E* and *F*). Importantly, in accordance with earlier studies (28), $Z_{HER2:342}$ and trastuzumab could bind simultaneously to SKOV-3 cells without blocking each other's binding sites (data not shown) confirming that they bind to different epitopes on HER2 (31). Furthermore, $Z_{HER2:342}$ and trastuzumab were used for traditional immunohistochemical staining of cryosections of SKOV-3 xenograft tumor tissues. Both the Affibody molecule and trastuzumab bound to SKOV-3 tumor cells leaving the surrounding and transversing mouse connective tissue negative (Fig. 3*G* and *H*) with no qualitative difference in the staining behavior between $Z_{HER2:342}$ and trastuzumab.

***In vivo* biodistribution.** To investigate whether improved affinity would result in improved tumor uptake, the affinity-matured $Z_{HER2:342}$ Affibody molecule ($K_D$ ~22 pmol/L) was compared with the first-generation Affibody molecule in its monovalent ($Z_{HER2:4}$, $K_D$ ~50 nmol/L for HER2) and divalent forms ($K_D$ ~3 nmol/L). Mice carrying SKOV-3 xenografts of ~3 mm in diameter were injected with $^{125}$I-labeled Affibody molecules. The radioactivity in excised tumors was measured at 1, 4, and 24 hours post-injection. and presented as the percentage of injected dose per gram of tissue (% ID/g; Table 1). Very little difference was observed between the two variants of the first-generation binder whereas the uptake for $Z_{HER2:342}$ compared with the parental $Z_{HER2:4}$ monomer was improved by 2.03, 3.94, and 24.29 times at 1, 4, and 24 hours, respectively, with a tumor uptake of ~9% ID/g at 4 hours (Fig. 4*A*). To verify that the observed tumor-targeting effect was indeed target mediated, one group of mice was pretreated with a 1,000-fold (0.5 mg) excess of unlabeled $Z_{HER2:342}$ Affibody molecule before injection of radiolabeled $Z_{HER2:342}$ Affibody molecule. Tumor uptake at 4 hours post-injection was reduced from 9.5 ± 2.3% to 1.5 ± 1.5% ID/g ($P < 0.01$) by the pretreatment, demonstrating that tumor uptake was target-specific. The same confirmation of target specificity was obtained both for the monomeric and dimeric form of first-generation of Affibody molecules, where tumor uptake was significantly reduced by the injection of a large excess of unlabeled forms of the same peptide ($P < 0.001$ and $P < 0.01$, respectively). The only sites of nonspecific accumulation were the kidneys, which could be expected for proteins with a size significantly below renal filtration threshold. However, the radioactivity was rapidly washed out from the kidneys.

It was apparent that the ratio of uptake in tumor compared with other organs was improved with increased affinity when the radioactivity concentration in tumor and blood was compared over time for the different Affibody molecules (Fig. 4*B*; Table 1). In spite of the increased affinity of the dimer, the difference in tumor-to-blood ratio between the monomeric and dimeric variants of the first-generation binder was modest. In contrast, a dramatic improvement was found for the $Z_{HER2:342}$ Affibody molecule, showing an impressive tumor-to-blood ratio of 38:1 at 4 hours and 100:1 at 24 hours post-injection. At 4 hours post-injection, tumor-to-organ ratios for most other organs were at least 2-fold

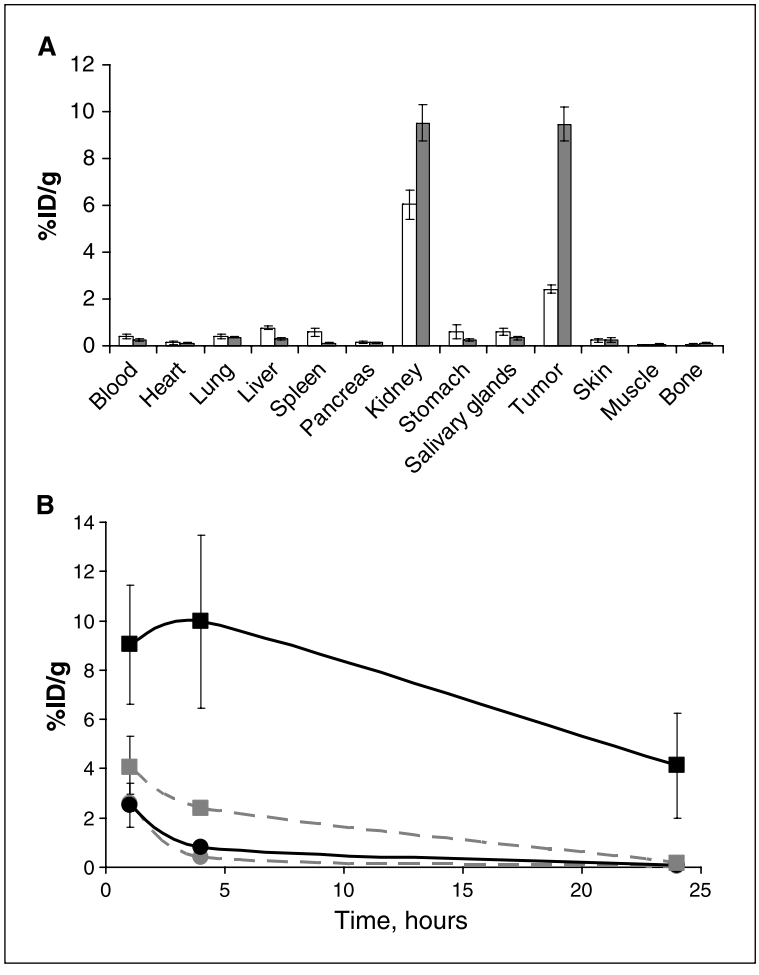


**Figure 4.** Evaluation of the Affibody molecules *in vivo*. *A,* biodistribution of $^{125}$I-labeled Affibody molecules 4 hours post-injection. Percentage of injected dose per gram of tissue is plotted for $Z_{HER2:4}$ (*white*), and $Z_{HER2:342}$ (*gray*), monovalent Affibody molecules (*columns,* mean; *bars,* ± SE; $n = 4$). *B,* in a second experiment, the relation in uptake between tumor and blood was investigated at different time points relevant to imaging; tumor (*squares*) and blood (*circles*) values for $Z_{HER2:4}$ (*dashed line*), and $Z_{HER2:342}$ (*solid line*). *Points,* mean; *bars,* ± SE ($n = 4$).

better for $Z_{HER2:342}$ in comparison with $Z_{HER2:4}$. Twenty-four hours post-injection, that difference was >10-fold. Furthermore, at 24 hours, the tumor to kidney ratio was improved to 9:1 for the $Z_{HER2:342}$ as compared with the $Z_{HER2:4}$, where the tumor to kidney ratio was 1:1.

**Gamma camera–based imaging of HER2 expression in SKOV-3 xenografts.** To evaluate whether the matured $Z_{HER2:342}$ could be used for *in vivo* imaging of HER2 expression, the Affibody molecule was labeled with $^{125}I$ and injected into mice carrying SKOV-3 tumors $\sim 0.5$ $cm^3$ in size. After 6 or 24 hours, images of tumor-bearing mice were acquired using a gamma camera. After 6 hours, the tumor could clearly be visualized with high contrast. At this time point, the only site with elevated radioactivity uptake besides the tumor were the kidneys. However, radioactivity accumulation in the tumor was appreciably higher than in the kidneys (Fig. 5*B*). The increase in contrast due to increase in affinity is striking when compared with the first-generation $(Z_{HER2:4})_2$ Affibody molecule, in which the kidney uptake is much more prominent than the tumor after 6 hours (Fig. 5*A*). After 24 hours, the nonspecific radioactivity accumulation was further reduced whereas a high dose remained on the tumor (Fig. 5*C*).

## Discussion

In this study, we describe *in vivo* tumor targeting by use of a new class of small affinity proteins called Affibody molecules. We reasoned that the very high affinity for the HER2 tumor target, combined with the very small size of the targeting molecule, may be an avenue for improving tumor specificity (39, 40)—and thus, the contrast of a radionuclide image—over existing larger affinity proteins like antibodies and fragments thereof (41, 42). To obtain small high affinity binders for HER2, a 6 kDa HER2-specific Affibody molecule was affinity maturated *in vitro*. The procedure used for affinity maturation resulted in an increased affinity by three orders of magnitude in one single maturation step. The matured Affibody molecule with highest affinity ($K_D$ of 22 pmol/L) was selected through various *in vitro* and *in vivo* characterizations and showed improved tumor targeting in biodistribution studies and gamma imaging.

It is interesting to compare the *in vivo* data of the $Z_{HER2:342}$ Affibody molecule described in this study with published results for other HER2-targeting proteins. We have restricted ourselves to the analysis of targeting of HER2 using radioiodinated proteins. Moreover, all studies which were selected for comparison used SKOV-3 ovarian carcinoma xenografts, the same as that used in this study. Together, this should minimize differences in agent-target interaction, antigen density, and cellular processing. Comparisons in the literature show that the uptake of the $Z_{HER2:342}$ Affibody molecule at 4 hours post-injection ($9.5 \pm 1.6\%$, ID/g) was similar to the uptake in tumor of the C6.5 scFv diabody (10.1% ID/g; ref. 43), and exceeded the uptake of the 741F8-2 sFv (2.9% ID/g; ref. 44), and its homodimer (5.6% ID/g; ref. 45). However, better clearance of $Z_{HER2:342}$ provided tumor-to-blood ratios, which at this time point, was 7.8 times better than for the C6.5 scFv diabody, 4.5 times better than for the 741F8-2 sFv, and 9.3 times better than for the 741F8-2 $(sFv')_2$. Advantages in contrast remained over time even at 24 hours.

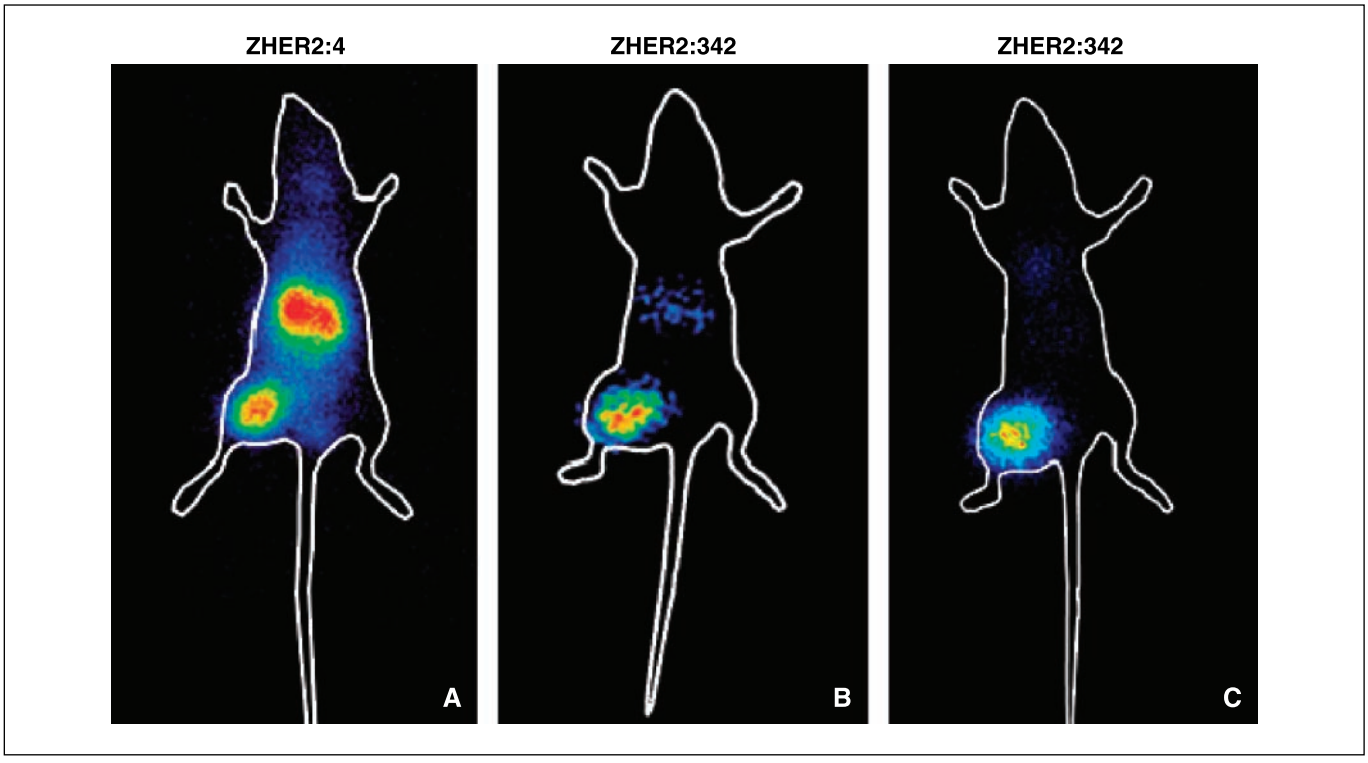


**Figure 5.** Gamma camera–based imaging of xenografted mice, at 6 and 24 hours after injection of $^{125}I$-labeled Affibody molecules. In a set of experiments, the first-generation Affibody molecule, $Z_{HER2:4}$ (*A*) was compared with the affinity-matured Affibody molecule $Z_{HER2:342}$ (*B*) at 6 hours post-injection. Intensity of color corresponds to radioactive accumulation: low (*blue*) and high (*yellow*) accumulation. Kidney uptake is more prominent for the $Z_{HER2:4}$ Affibody molecule (*A*). The tumor uptake of $Z_{HER2:342}$ was stable up to at least 24 hours post-injection (*C*).

It has been suggested that bivalently binding antibody fragments have superior tumor specificity compared with their monovalent counterparts (46), and in a recent study, Wu and colleagues showed that even relatively large (~80 kDa) HER2-specific divalent minibodies could be used for tumor imaging in mice (47). However, a bivalent antibody fragment is, by necessity, larger than a monovalent one, and should thus have poorer tissue penetration properties (39). It remains an open question if the targeting benefit of divalency could be overcome by increased affinity for a monovalent smaller fragment. In this study, the first-generation bivalent HER2 Affibody molecule ($K_D$ 3 nmol/L) did not show improved tumor-to-blood ratios compared with the monovalent molecule ($K_D$ 50 nmol/L), in spite of higher affinity. In contrast, when improving the affinity, both the total tumor uptake and tumor-to-blood contrast improved dramatically. These results may suggest that for very small proteins, keeping the size small is more important than gaining functional affinity by dimerization.

Taken together, these results suggest that the radioiodinated $Z_{HER2:342}$ Affibody molecule may be a suitable agent for *in vivo* imaging of HER2 expression, and a literature comparison suggests that $Z_{HER2:342}$ may provide better tumor contrast at early time points than HER2-specific antibodies and fragments thereof (48). It is important to choose the optimal time point for the image, as there is an initial high uptake of activity in the kidneys due to excretion. The activity is, however, rapidly decreasing, from almost 50% ID/g at 1 hour post-injection to <10% ID/g at 4 hours post-injection. Six hours post-injection, the uptake in the tumor is much more prominent than the kidneys, as can be seen in Fig. 5*B*.

If the molecule was to be tested in the clinic, obviously a single-photon emitter $^{123}I$ ($T_{1/2}$ = 13.3 hours) or positron-emitter $^{124}I$ ($T_{1/2}$ = 4.17 days) should be used instead of $^{125}I$. The development of suitable chemistry to label the $Z_{HER2:342}$ molecule with generator-produced $^{99m}Tc$ ($T_{1/2}$ = 6 hours) or $^{68}Ga$ ($T_{1/2}$ = 68 minutes) could further facilitate future imaging studies.

## Acknowledgments

Received 10/6/2005; revised 12/19/2005; accepted 2/13/2006.

**Grant support:** P25882-1 from the Swedish Agency for Innovation Systems (VINNOVA) and by two research grants from the Swedish Cancer Society.

The costs of publication of this article were defrayed in part by the payment of page charges. This article must therefore be hereby marked *advertisement* in accordance with 18 U.S.C. Section 1734 solely to indicate this fact.

We thank Per-Åke Nygren and Elin Gunneriusson for valuable advice on the affinity maturation, Per-Olof Fjällström for computing the software for clustering of selected clones, and Lars Abrahmsén and Birger Jansson for comments on the manuscript.



## References

1. Behr TM, Gotthardt M, Barth A, Behe M. Imaging tumors with peptide-based radioligands. Q J Nucl Med 2001;45:189–200.
2. Britz-Cunningham SH, Adelstein SJ. Molecular targeting with radionuclides: state of the science. Nucl Med 2003;44:1945–61.
3. Santimaria M, Moscatelli G, Viale GL, et al. Immunoscintigraphic detection of the ED-B domain of fibronectin, a marker of angiogenesis, in patients with cancer. Clin Cancer Res2003;9:571–9.
4. Olafsen T, Kenanova VE, Sundaresan G, et al. Optimizing radiolabeled engineered anti-p185HER2 antibody fragments for *in vivo* imaging. Cancer Res 2005;65:5907–16.
5. Robinson MK, Doss M, Shaller C, et al. Quantitative immuno-positron emission tomography imaging of HER2-positive tumor xenografts with an iodine-124 labeled anti-HER2 diabody. Cancer Res 2005;65: 471–8.
6. Michel CC, Curry FE. Microvascular permeability [review]. Physiol Rev 1999;79:703–61.
7. Heppler A, Froidevaux S, Eberle AN, Maecke H. Receptor targeting for tumor localization and therapy with radiopeptides. Curr Med Chem 2000;7:791–4.
8. Reubi JC. Somatostatin and other peptide receptors as tools for tumor diagnosis and treatment. Neuroendocrinology 2004;80:51–6.
9. Landon LA, Deutscher SL. Combinatorial discovery of tumor targeting peptides using phage display. J Cell Biochem 2003;90:509–17.
10. Nygren PA, Skerra A. Binding proteins from alternative scaffolds [review]. J Immunol Methods 2004;290:3–28.
11. Skerra A. Engineered protein scaffolds for molecular recognition. J Mol Recognit 2001;13:167–87. Review Erratum in: J Mol Recognit 2001;14:141.
12. Binz HK, Amstutz P, Pluckthun A. Engineering novel binding proteins from nonimmunoglobulin domains. Nat Biotechnol 2005;23:1257–68.
13. Xu L, Aha P, Gu K, et al. Directed evolution of high-affinity antibody mimics using mRNA display. Chem Biol 2002;9:933–42.
14. Koide A, Abbatiello S, Rothgery L, Koide S. Probing protein conformational changes in living cells by using designer binding proteins: application to the estrogen receptor. Proc Natl Acad Sci U S A 2002;99:1253–8.
15. Skerra A. Lipocalins as a scaffold [review]. Biochim Biophys Acta 2000;1482:337–50.
16. Binz HK, Amstutz P, Kohl A, et al. High-affinity binders selected from designed ankyrin repeat protein libraries. Nat Biotechnol 2004;22:575–82.
17. Li Y, Moysey R, Molloy PE, et al. Directed evolution of human T-cell receptors with picomolar affinities by phage display. Nat Biotechnol 2005;23:349–54.
18. Nord K, Gunneriusson E, Ringdahl J, Stahl S, Uhlen M, Nygren PA. Binding proteins selected from combinatorial libraries of an α-helical bacterial receptor domain. Nat Biotechnol 1997;15:772–7.
19. Ronnmark J, Gronlund H, Uhlen M, Nygren PA. Human immunoglobulin A (IgA)-specific ligands from combinatorial engineering of protein A. Eur J Biochem 2002;269:2647–55.
20. Ronnmark J, Hansson M, Nguyen T, et al. Construction and characterization of affibody-Fc chimeras produced in *Escherichia coli*. J Immunol Methods 2002;261:199–211.
21. Sandstrom K, Xu Z, Forsberg G, Nygren PA. Inhibition of the CD28–CD80 co-stimulation signal by a CD28-binding Affibody ligand developed by combinatorial protein engineering. Protein Eng 2003;16:691–7.
22. Natali PG, Nicotra MR, Bigotti A, et al. Expression of the p185 encoded by HER2 oncogene in normal and transformed human tissues. Int J Cancer 1990;45:457–61.
23. Press MF, Cordon-Cardo C, Slamon DJ. Expression of the HER2/neu proto-oncogene in normal human adult and fetal tissues. Oncogene 1990;5:953–62.
24. Wang SC, Zhang L, Hortobagyi GN, Hung MC. Targeting HER2: recent developments and future directions for breast cancer patients [review]. Semin Oncol 2001;28:21–9.
25. Gancberg D, Di Leo A, Cardoso F, et al. Comparison of HER2 status between primary breast cancer and corresponding distant metastatic sites. Ann Oncol 2002; 13:1036–43.
26. Carlsson J, Nordgren H, Sjostrom J, et al. HER2 expression in breast cancer primary tumours and corresponding metastases. Original data and literature review [review]. Br J Cancer 2004;90:2344–8.
27. Bast RC, Jr., Ravdin P, Hayes DF, et al. American Society of Clinical Oncology Tumor Markers Expert Panel. 2000 update of recommendations for the use of tumor markers in breast and colorectal cancer: clinical practice guidelines of the American Society of Clinical Oncology. J Clin Oncol 2001;19:1865–78. Erratum in: J. Clin. Oncol. 2001;19:4185–8 and J Clin Oncol 2002;20: 2213.
28. Wikman M, Steffen AC, Gunneriusson E, et al. Selection and characterization of HER2/neu-binding Affibody ligands. Protein Eng Des Sel 2004;17:455–62.
29. Kuan CT, Wikstrand CJ, Archer G, et al. Increased binding affinity enhances targeting of glioma xenografts by EGFRvIII-specific scFv. Int J Cancer 2000;88: 962–9.
30. Adams GP, Schier R, Marshall K, et al. Increased affinity leads to improved selective tumor delivery of single-chain Fv antibodies. Cancer Res 1998;58:485–90.
31. Steffen AC, Wikman M, Tolmachev V, et al. *In vitro* characterization of a bivalent anti-HER2 Affibody with potential for radionuclide-based diagnostics. Cancer Biother Radiopharm 2005;20:239–48.
32. Steffen AC, Orlova A, Wikman M, et al. Affibody-mediated tumour targeting of HER-2–expressing xenografts in mice. Eur J Nucl Med Mol Imaging. 2006 Mar 15 [Epub ahead of print].
33. Schier R, McCall A, Adams GP, et al. Isolation of picomolar affinity anti-c-erbB-2 single-chain Fv by molecular evolution of the complementarity determining regions in the center of the antibody binding site. J Mol Biol 1996;263:551–67.
34. Rüther U. pUR 250 allows rapid chemical sequencing of both DNA strands of its inserts. Nucleic Acids Res 1982;10:5765–72.
35. Horak EM, Heitner T, Garrison JL, et al. Engineering bispecific single-chain Fv molecules to alter signaling of the EGF receptor family. Proc Am Assoc Cancer Res 2001;42:774.
36. Gunneriusson E, Nord K, Uhlen M, Nygren P. Affinity maturation of a Taq DNA polymerase specific Affibody by helix shuffling. Protein Eng 1999;12:873–8.
37. Nord K, Nord O, Uhlen M, Kelley B, Ljungqvist C, Nygren PA. Recombinant human factor VIII-specific affinity ligands selected from phage-displayed combinatorial libraries of protein A. Eur J Biochem 2001;268: 4269–77.
38. Nilsson J, Larsson M, Stahl S, Nygren PA, Uhlen M. Multiple affinity domains for the detection, purification and immobilization of recombinant proteins. J Mol Recognit 1996;9:585–94.
39. Yokota T, Milenic DE, Whitlow M, Schlom J. Rapid tumor penetration of a single-chain Fv and comparison with other immunoglobulin forms. Cancer Res 1992;52: 3402–8.

**40.** Batra SK, Jain M, Wittel UA, Chauhan SC, Colcher D. Pharmacokinetics and biodistribution of genetically engineered antibodies. Curr Opin Biotechnol 2002;13: 603–8.

**41.** Holt LJ, Herring C, Jespers LS, Woolven BP, Tomlinson IM. Domain antibodies: proteins for therapy [review]. Trends Biotechnol 2003;21:484–90.

**42.** Cortez-Retamozo V, Lauwereys M, Hassanzadeh Gh G, et al. Efficient tumor targeting by single-domain antibody fragments of camels. Int J Cancer 2002;98: 456–62.

**43.** Adams GP, Schier R, McCall AM, et al. Prolonged *in vivo* tumour retention of a human diabody targeting the extracellular domain of human HER2/neu. Br J Cancer 1998;77:1405–12.

**44.** Adams GP, McCartney JE, Tai MS, et al. Highly specific *in vivo* tumor targeting by monovalent and divalent forms of 741F8 anti-c-erbB-2 single-chain Fv. Cancer Res 1993;53:4026–34.

**45.** Tai MS, McCartney JE, Adams GP, et al. Targeting c-erbB-2 expressing tumors using single-chain Fv monomers and dimers. Cancer Res 1995;55:5983s–9s.

**46.** Nielsen UB, Adams GP, Weiner LM, Marks JD. Targeting of bivalent anti-ErbB2 diabody antibody fragments to tumor cells is independent of the intrinsic antibody affinity. Cancer Res 2000;60:6434–40.

**47.** Olafsen T, Kenanova VE, Sundaresan G, et al. Optimizing radiolabeled engineered anti-p185$^{-HER2}$ antibody fragments for *in vivo* imaging. Cancer Res 2005;65:5907–16.

**48.** Smith-Jones PM, Solit DB, Akhurst T, et al. Imaging the pharmacodynamics of HER2 degradation in response to Hsp90 inhibitors. Nat Biotechnol 2004;22:701–6.